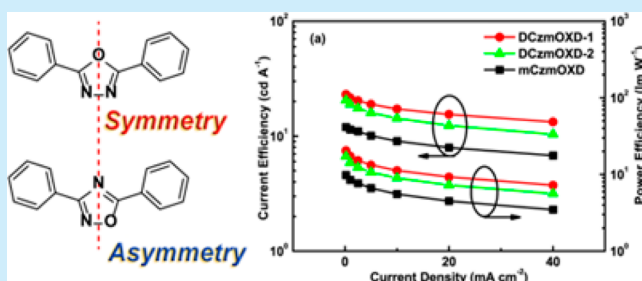


Asymmetric Design of Bipolar Host Materials with Novel 1,2,4-Oxadiazole Unit in Blue Phosphorescent Device

Qian Li,[†] Lin-Song Cui,[†] Cheng Zhong,[‡] Zuo-Quan Jiang,^{*,†} and Liang-Sheng Liao^{*,†}[†]Jiangsu Key Laboratory for Carbon-Based Functional Materials & Devices, Institute of Functional Nano & Soft Materials (FUNSOM) & Collaborative Innovation Center of Suzhou Nano Science and Technology, Soochow University, Suzhou 215123, P.R. China[‡]Department of Chemistry, Hubei Key Lab on Organic and Polymeric Optoelectronic Materials, Wuhan University, Wuhan 430072, P.R. China

S Supporting Information

ABSTRACT: The intrinsic asymmetry of 1,2,4-oxadiazole was utilized to synthesize three isomers, DCzmOXD-1, DCzmOXD-2, and mCzmOXD, and high triplet energies over 2.80 eV made them good candidates for host materials in blue OLEDs. The best efficiencies of 23.0 cd A⁻¹/20.5 lm W⁻¹/11.2% in CE/PE/EQE were achieved by DCzmOXD-1 with derivation at the β -carbon position of 1,2,4-oxadiazole.



During the past decades, there has been growing interest in developing new organic π -conjugated materials for optoelectronic devices, such as organic light-emitting diodes (OLEDs), organic field-effect transistors (OFETs), and organic photovoltaics (OPVs).¹ In this development, organic synthesis plays a pivotal role in constructing various p-type or n-type functional materials.² Molecular engineering gave organic chemists many means such as the modification of backbones, side chains, substituents, linking positions, etc. to modulate the material properties.³ In this way, numerous classic π -conjugated units and their derivatives (for instance, fluorene, carbazole, naphthalene, pentacene, perylene, thiophene, 1,3,4-oxadiazole, etc.) have been investigated and applied in different areas.⁴ It should be noted that most of these classic units are symmetrical units. An additional option in molecular engineering could be employed if people can develop some asymmetry units, because the properties will vary with the change of substituted position or direction. For example, G. Bazan's group systematically studied an asymmetrical unit 4,7-dibromo[1,2,5]thiadiazolo[3,4-*c*]pyridine and found that the critical HOMO/LUMO levels of the resulted small molecules could be finely tuned by adopting a different configuration with the same substituents.⁵ Recently, we also reported a new asymmetrical π -conjugated unit 1,2,4-oxadiazole, an isomer of 1,3,4-oxadiazole, and its application as host materials in phosphorescent OLEDs (PHOLEDs).⁶ It is known that the PHOLEDs have great potential in achieving a high internal quantum efficiency of $\sim 100\%$ by harvesting both singlet and triplet excitons.⁷ The phosphor emitters should be doped uniformly in the host materials to suppress the multiparticle quenching effects. The first design principle of host materials is that the triplet energy of the host should be higher than that of the emitting phosphor.

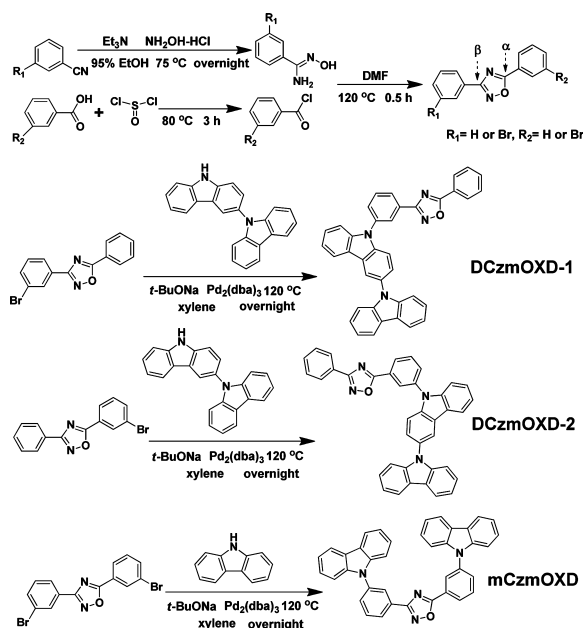
In this regard, the conjugation size of a host molecule should be confined and the meta-linkage is undoubtedly a good choice.⁸ Previously, we wanted to utilize the *meta*-linked configuration of 1,2,4-oxadiazole to increase the triplet energy (as compared to its 1,3,4-isomer) in our design which was successful; the resulting mCzmOXD could gain a triplet energy of 2.81 eV and achieve a current efficiency of 11.5 cd A⁻¹ in blue phosphorescent OLEDs. During this research process, we gradually realize that the asymmetry of 1,2,4-oxadiazole could be another factor to influence the material property. In this work, we rearranged the building blocks and synthesized two new host materials DCzmOXD-1 and DCzmOXD-2 in asymmetrical design, which could achieve enhanced current efficiencies of 22.5 and 19.9 cd A⁻¹, respectively.

Synthetic routes of the three compounds are outlined in Scheme 1. The 1,2,4-oxadiazole rings are formed from the corresponding amidoximes and acylchlorides. Then the resulted 1,2,4-oxadiazole derivatives were reacted with carbazole or 9H-3,9'-bicarbazole to obtain the final products by Buchwald–Hartwig reaction.⁹ All the materials are fully characterized, and their thermal properties were determined by differential scanning calorimetry (DSC) and thermogravimetric analysis (TGA) measurements (Supporting Information (SI)). As shown in Table 1 and Figure S7, all the materials exhibited high glass-transition temperatures over 100 °C, which indicated good thermal and morphological stability under device fabrication.

Received: January 23, 2014

Published: March 3, 2014

Scheme 1. Synthetic Routes and Chemical Structures of the Materials



The ambipolar behaviors of DCzmOXD-1, DCzmOXD-2, and mCzmOXD were probed by cyclic voltammetry (see Table 1 and SI). The cyclic voltammogram curves suggest the bipolar transporting properties in the three materials. As summarized in Table 1, the HOMO and LUMO levels of the three compounds are 5.99, 5.64, and 5.80 eV (HOMO), and 2.47, 2.26, and 2.48 eV (LUMO), respectively.

To further understand the structure–property relationship of the compounds and explain the orbital energy data in Table 1, the electronic properties of the compounds were studied by density functional theory (DFT) calculations at the B3LYP/6-31g(d) level.¹⁰ As shown in Figure 1, the HOMO of mCzmOXD localized at the phenyl carbazole unit near the β -carbon while the LUMO localized on the diphenyl oxadiazole unit. It could be understood as follows: First, due to the meta-substitution configuration, the conjugation between the two groups, connected at α -carbon and β -carbon, is less effective. Second, the central 1,2-oxadiazole ring exerts more of an electron-withdrawing effect on the α -carbon than the β -carbon, because of the more effective conjugation and larger frontier orbital distribution on the α -carbon. This phenomenon gives further contribution to the HOMO–LUMO separation in mCzmOXD, which is also observed in DCzmOXD-1 and DCzmOXD-2. DCzmOXD-1 possessed higher HOMO and LUMO energy levels, as well as a more evident separation of HOMO and LUMO compared to DCzmOXD-2, because of

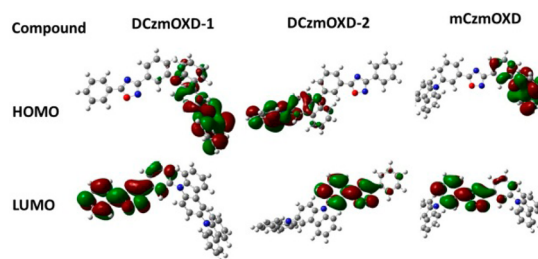


Figure 1. Optimized geometry and HOMO/LUMO spatial distributions of DCzmOXD-1, DCzmOXD-2, and mCzmOXD.

the 3,9'-bicarbazole group is appended to the phenyl ring at the β -carbon, which has a relatively lower electron withdrawing effect.

Figure 2 depicts the UV–vis absorption of the three compounds in dichloromethane (CH_2Cl_2) and the photo-

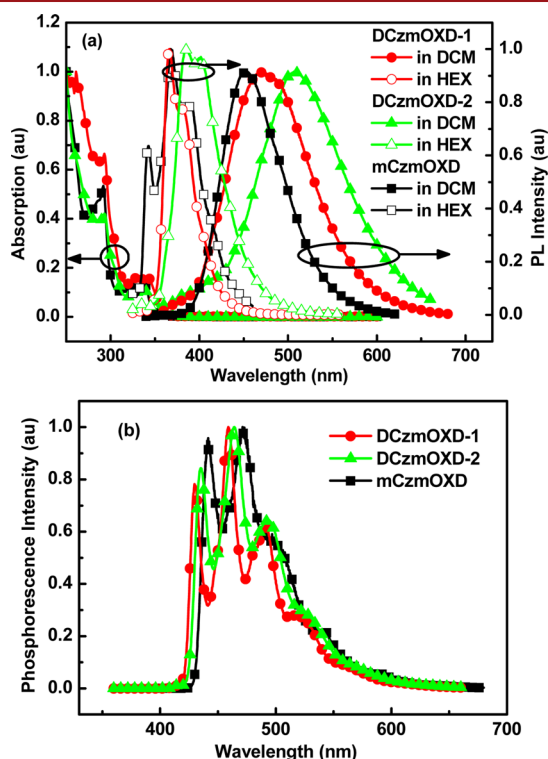


Figure 2. (a) UV–vis absorption in dichloromethane and PL spectra in dichloromethane and *n*-hexane solution at 10^{-5} M. (b) Phosphorescence spectra of these compounds measured in a frozen 2-methyltetrahydrofuran matrix at 77 K.

Table 1. Physical Properties of DCzmOXD-1, DCzmOXD-2, and mCzmOXD

compd	T_g^a ($^\circ\text{C}$)	T_d^a ($^\circ\text{C}$)	$\lambda_{\text{max,abs}}^b$ (nm)	$\lambda_{\text{max,f}}^b$ (nm)	λ_{ph}^c (nm)	E_g^d (eV)	E_T^e (eV)	HOMO/LUMO ^f (eV)
DCzmOXD-1	110	341	293, 342	367, 385	430	3.38	2.88	5.64/2.26
DCzmOXD-2	114	334	295, 339	340, 370, 392	435	3.32	2.85	5.80/2.48
mCzmOXD	100	362	291, 337	385, 400	442	3.52	2.81	5.99/2.47

^a T_g : glass transition temperatures, T_d : decomposition temperatures; measured by DSC and TGA. ^bUV–vis absorptions were measured in dichloromethane solution at rt, and PL spectra were measured in *n*-hexane solution at rt. ^cMeasured in 2-MeTHF glass matrix at 77 K. ^d E_g : The band gap energy was estimated from the optical absorption edges of UV–vis absorption spectra. ^e E_T : The triplet energy was estimated from the onset peak of the phosphorescence spectra. ^fHOMO and LUMO estimated from the onset of oxidation potentials and the optical band gap from the absorption spectra.

luminescence (PL) spectra in dichloromethane and *n*-hexane at rt; all the results are summarized in Table 1. The absorption around 296 nm for all the compounds has an affirmative similarity to that of the unsubstituted carbazole. The optical band gap energies of DCzmOXD-1, DCzmOXD-2, and mCzmOXD calculated from the threshold of the absorption spectra in CH₂Cl₂ solution are 3.38, 3.32, and 3.52 eV, respectively. The emissions of the compounds DCzmOXD-1, DCzmOXD-2, and mCzmOXD in hexane solution are in the range 390–442 nm. Evidently, DCzmOXD-1 exhibited hypsochromic emission by 52 nm in comparison with its counterpart DCzmOXD-2, which is because of the fact that the conjugation of the β -carbon with 1,2,4-oxadiazole is weaker than the α -carbon of 1,2,4-oxadiazole. But all the compounds showed significant red shifts in CH₂Cl₂ solution for the typical photoinduced intramolecular charge transfer (Figure S11). The phosphorescence spectra were measured in a frozen 2-methyltetrahydrofuran matrix at 77 K, and the triplet energy levels were estimated from the highest-energy vibronic subband of the phosphorescence spectra. To our satisfaction, the E_T of all three compounds are about 2.8 eV, which is higher than that of the most popular sky-blue emitter iridium(III) bis(4,6-(difluorophenyl)pyridinato-*N,C'*)picolinate (FIrpic). The above phenomena could be attributed to the suppression of intramolecular charge transfer transition because of the meta-phenyl linkage and limited conjugation via the 1,2,4-oxadiazole ring. This can also be proved by the comparison with the 1,3,4-oxadiazole derivatives which have a relatively low E_T of ~2.6 eV.¹¹ Based on these results, DCzmOXD-1, DCzmOXD-2, and mCzmOXD proved to possess sufficiently high E_T to serve as host materials for blue PHOLEDs.

To further investigate the electroluminescent properties of the materials, OLEDs with the structure of indium tin oxide (ITO)/molybdenum trioxide: 1,3-di(9H-carbazol-9-yl)benzene (MoO₃: mCP) (45 nm)/mCP (10 nm)/Host: FIrpic (25 nm, 8 wt %)/1,3,5-tri[(3-pyridyl)-phen-3-yl]benzene (TmPyPB) (30 nm)/8-hydroxyquinolitolithium (Liq) (2 nm)/Al (120 nm) (Host = DCzmOXD-1: device A; DCzmOXD-2: device B; mCzmOXD: device C) were fabricated. MoO₃: mCP was used as the hole-injection layer (HIL), mCP was used as the hole transport layer (HTL) and electron blocking layer (EBL); DCzmOXD-1, DCzmOXD-2, and mCzmOXD, doped with FIrpic, were used as the emitting layers (EML); TmPyPB was used as the hole-blocking layer (HBL); Liq was used as electron-injecting layer (EIL); and Al was used as cathode.

Figure 3 shows the EL efficiencies and current–voltage–luminescence (*J*–*V*–*L*) characteristics of the devices. The EL spectra of the devices (see SI) show the identical spectra with a peak at 472 nm and a shoulder at 500 nm; this means that only the FIrpic emission peak was observed without any emission from DCzmOXD-1, DCzmOXD-2. Such a finding strongly indicated that the emissive excitons and charges were efficiently confined inside the emitting layer. It could be attributed to the high triplet energies (above 2.8 eV) of the three host materials. As listed in Table 2, the driving voltages at 100 cd m^{−2} are 3.6, 3.9, and 4.2 V for the DCzmOXD-1, DCzmOXD-2, and mCzmOXD based devices, respectively. This declared that the driving voltages of device A and B were about 0.6 and 0.3 eV lower than that of device C and the lowest driving voltage can be obtained from device A. The maximum current efficiency and current efficiency at 100 cd m^{−2} of device A were 23.0 and 22.5 cd A^{−1}, while the corresponding values obtained from device B were 19.9 and 16.0 cd A^{−1}. The efficiencies of the

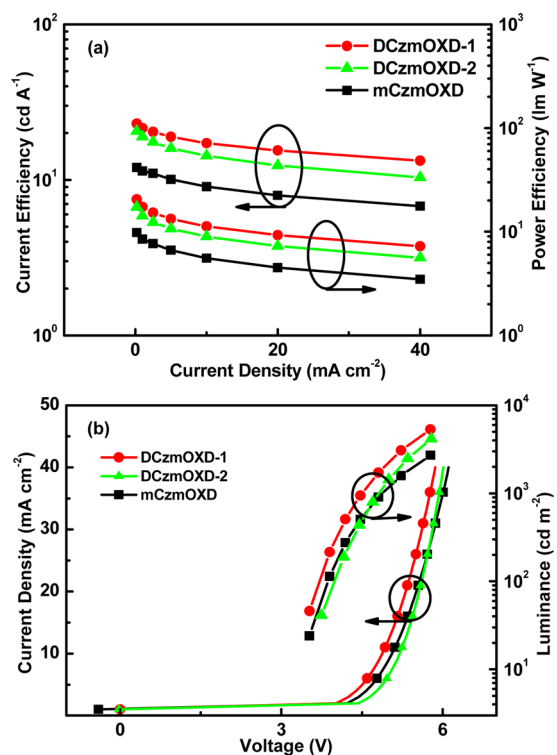


Figure 3. (a) Current efficiency and power efficiency versus current density curves; (b) Current density–voltage–luminescence characteristics.

Table 2. Electroluminescence Data of the FIrpic-Based Blue Devices

	host	$\eta_c/\eta_p/\eta_{ext}/V^a$ (cd A ^{−1} /lm W ^{−1} / %/ V)			
		$\eta_{c\ max}/\eta_{p\ max}/\eta_{ext\ max}/V^b$ (cd A ^{−1} /lm W ^{−1} / %/ V)			
A	DCzmOXD-1	22.5/19.6/8.3/3.6	23.0/20.5/11.2/3.5		
B	DCzmOXD-2	19.9/16.0/8.6/3.9	20.5/17.2/9.7/3.7		
C	mCzmOXD	11.5/8.6/5.0/4.2	12.0/9.8/5.8/3.8		

^aCurrent efficiency (η_c), power efficiency (η_p), external quantum efficiency (η_{ext}), voltage (V) at 100 cd m^{−2}. ^bMaximum current efficiency ($\eta_{c\ max}$), power efficiency ($\eta_{p\ max}$), and external quantum efficiency ($\eta_{ext\ max}$).

DCzmOXD-1 and DCzmOXD-2 devices were much higher than those of the mCzmOXD device (11.5 cd A^{−1}, 8.6 cd A^{−1}@ 100 cd m^{−2}). This may be because in device A and B the hole charge are more effectively trapped on FIrpic which can lead to direct charge recombination.¹² The resulting lower driving voltage at the same current density observed in device A also supported this expatiation. In addition to that, the efficiencies of device A and B were more stable than that of device C. The CIE coordinate for all the devices at 4 V is (0.16, 0.37), with only small CIE shifts with the change of voltage.

In summary, we have designed and synthesized a new series of 1,2,4-oxadiazole-based host materials DCzmOXD-1, DCzmOXD-2, and mCzmOXD. To date, most work on oxadiazole derivatives in OLED applications always surrounding the 1,3,4-oxadiazole, but the 1,2,4-isomer has its unique merit. Benefiting from the *meta*-linkage of 1,2,4-oxadiazole, we could combine it with electron-donating carbazole units as bipolar materials and then utilize them in blue phosphorescent organic light-emitting devices due to their high triplet energies. Moreover, the intrinsic asymmetry of 1,2,4-oxadiazole is very

important in molecular design. Modification on the α - or β -carbon position will bring different properties in energy levels. Finally, the best performances of 23.0 cd A⁻¹/20.5 lm W⁻¹/11.2% in CE/PE/EQE were achieved when DCzmOXD-1 was used as a blue host material in device evaluation. These results are obviously better than those of mCzmOXD, which is derived from both sides of 1,2,4-oxadiazole.

■ ASSOCIATED CONTENT

■ Supporting Information

Synthesis, UV-vis, FL, NMR, EL, references. This material is available free of charge via the Internet at <http://pubs.acs.org>.

■ AUTHOR INFORMATION

Corresponding Authors

*E-mail: zqjiang@suda.edu.cn.

*E-mail: lsiao@suda.edu.cn.

Notes

The authors declare no competing financial interest.

■ ACKNOWLEDGMENTS

We are grateful for the financial support from the Natural Science Foundation of China (Nos. 21202114, 21161160446, 61036009, and 61177016). This project is also supported by the Fund for Excellent Creative Research Teams of Jiangsu Higher Education Institutions.

■ REFERENCES

- (1) (a) Tao, Y.-T.; Yang, C.-L.; Qin, J.-G. *Chem. Soc. Rev.* **2011**, *40*, 2943. (b) Murphy, A. R.; Fréchet, J. M. J. *Chem. Rev.* **2007**, *107*, 1066. (c) Hains, A. W.; Liang, Z.; Woodhouse, M. A.; Gregg, B. A. *Chem. Rev.* **2010**, *110*, 6689. (d) Wong, W.-Y.; Ho, C.-L. *Acc. Chem. Res.* **2010**, *43*, 1246. (e) Wong, W.-Y.; Ho, C.-L. *New J. Chem.* **2013**, *37*, 1665. (f) Zhang, Y.; Haske, W.; Cai, D.; Barlow, S.; Kippelen, B.; Marder, S. R. *RSC Adv.* **2013**, *3*, 23514.
- (2) Zhao, Y.; Guo, Y.; Liu, Y. *Adv. Mater.* **2013**, *25*, 5372.
- (3) (a) Wang, Q.; Ma, D. *Chem. Soc. Rev.* **2010**, *39*, 2387. (b) Cai, J.-X.; Ye, T.-L.; Fan, X.-F.; Han, C.-M.; Xu, H.; Wang, L.-L.; Ma, D.-G.; Lin, Y.; Yan, P.-F. *J. Mater. Chem.* **2011**, *21*, 15405.
- (4) (a) Chen, L.; Mahmoud, S. M.; Yin, X.; Lalancette, R. A.; Pietrangelo, A. *Org. Lett.* **2013**, *15*, 5970. (b) Salman, S.; Kim, D.; Coropceanu, V.; Brédas, J.-L. *Chem. Mater.* **2011**, *23*, 5223. (c) Banerjee, A.; Basak, S.; Nanda, J. *Chem. Commun.* **2013**, *49*, 6891. (d) Wang, M.; Li, J.; Zhao, G.; Wu, Q.; Huang, Y.; Hu, W.; Gao, X.; Li, H.; Zhu, D. *Adv. Mater.* **2013**, *25*, 2229. (e) Luo, J.; Xu, M.; Li, R.; Huang, K.-W.; Jiang, C.; Qi, Q.; Zeng, W.; Zhang, J.; Chi, C.; Wang, P.; Wu, J. *J. Am. Chem. Soc.* **2013**, *136*, 265. (f) Leung, M.-K.; Yang, W.-H.; Chuang, C.-N.; Lee, J.-H.; Lin, C.-F.; Wei, M.-K.; Liu, Y.-H. *Org. Lett.* **2012**, *14*, 4986.
- (5) Coughlin, J. E.; Henson, Z. B.; Welch, G. C.; Bazan, G. C. *Acc. Chem. Res.* **2014**, *47*, 257.
- (6) Li, Q.; Cui, L.-S.; Zhong, C.; Yuan, X.-D.; Dong, S.-C.; Jiang, Z.-Q.; Liao, L.-S. *Dyes Pigm.* **2013**, *101*, 142.
- (7) (a) Baldo, M. A.; O'Brien, D.; You, F. Y.; Shoustikov, A.; Sibley, S.; Thompson, M. E.; Forrest, S. R. *Nature* **1998**, *395*, 151. (b) Groves, C. *Nat. Mater.* **2013**, *12*, 597. (c) Ma, Y.; Zhang, H.; Shen, J.; Che, C. *Synth. Met.* **1998**, *94*, 245. (d) Reineke, S.; Lindner, F.; Schwartz, G.; Seidler, N.; Walzer, K.; Lussem, B.; Leo, K. *Nature* **2009**, *459*, 234. (e) Seo, J. H.; Lee, S. J.; Seo, B. M.; Moon, S. J.; Lee, K. H.; Park, J. K.; Yoon, S. S.; Kim, Y. K. *Org. Electron.* **2010**, *11*, 1759. (f) Xiao, L.; Chen, Z.; Qu, B.; Luo, J.; Kong, S.; Gong, Q.; Kido, J. *Adv. Mater.* **2010**, *23*, 926. (g) Kim, M.; Lee, J. Y. *Chem.—Asian J.* **2012**, *7*, 899. (h) Wong, W.-Y.; Ho, C.-L. *J. Mater. Chem.* **2009**, *19*, 4457. (i) Wong, W.-Y.; Ho, C.-L. *Coord. Chem. Rev.* **2009**, *253*, 1709. (j) Wong, W.-Y.; Ho, C.-L. *Coord. Chem. Rev.* **2013**, *257*, 1614.
- (8) (a) Jeon, S. O.; Lee, J. Y. *J. Mater. Chem.* **2012**, *22*, 4233. (b) Dong, S.-C.; Gao, C.-H.; Yuan, X.-D.; Cui, L.-S.; Jiang, Z.-Q.; Lee, S.-T.; Liao, L.-S. *Org. Electron.* **2013**, *14*, 902. (c) Cui, L.-S.; Dong, S.-C.; Liu, Y.; Li, Q.; Jiang, Z.-Q.; Liao, L.-S. *J. Mater. Chem. C* **2013**, *1*, 3967.
- (9) US 2009/0134784 A1 2009-5-28.
- (10) Salman, S.; Kim, D.; Coropceanu, V.; Brédas, J.-L. *Chem. Mater.* **2011**, *23*, 5223.
- (11) Tao, Y.-T.; Wang, Q.; Yang, C.-L.; Zhong, C.; Zhang, K.; Qin, J.-G.; Ma, D.-G. *Adv. Funct. Mater.* **2010**, *20*, 304.
- (12) Holmes, R. J.; Dandrade, B. W.; Forrest, S. R.; Ren, X.; Li, J.; Thompson, M. E. *Appl. Phys. Lett.* **2003**, *83*, 3818.